

S. Lissner, L. Nold, C.-J. Hsieh, J. R. Turner, M. Gregor, L. Graeve and G. Lamprecht

Am J Physiol Gastrointest Liver Physiol 299:907-920, 2010. First published Jul 15, 2010;
doi:10.1152/ajpgi.00191.2010

You might find this additional information useful...

This article cites 51 articles, 28 of which you can access free at:

<http://ajpgi.physiology.org/cgi/content/full/299/4/G907#BIBL>

Updated information and services including high-resolution figures, can be found at:

<http://ajpgi.physiology.org/cgi/content/full/299/4/G907>

Additional material and information about *AJP - Gastrointestinal and Liver Physiology* can be found at:

<http://www.the-aps.org/publications/ajpgi>

This information is current as of November 8, 2010 .

Activity and PI3-kinase dependent trafficking of the intestinal anion exchanger downregulated in adenoma depend on its PDZ interaction and on lipid rafts

S. Lissner,¹ L. Nold,¹ C.-J. Hsieh,¹ J. R. Turner,² M. Gregor,¹ L. Graeve,³ and G. Lamprecht¹

¹1st Medical Department, University of Tübingen, Tübingen, Germany, ²Department of Pathology, University of Chicago, Chicago, Illinois; and ³Department of Biological Chemistry and Nutrition, University of Hohenheim, Hohenheim, Germany

Submitted 22 April 2010; accepted in final form 14 July 2010

Lissner S, Nold L, Hsieh C-J, Turner JR, Gregor M, Graeve L, Lamprecht G. Activity and PI3-kinase dependent trafficking of the intestinal anion exchanger downregulated in adenoma depend on its PDZ interaction and on lipid rafts. *Am J Physiol Gastrointest Liver Physiol* 299: G907–G920, 2010. First published July 15, 2010; doi:10.1152/ajpgi.00191.2010.—The Cl/HCO₃ exchanger downregulated in adenoma (DRA) mediates electroneutral NaCl absorption in the intestine together with the apical Na/H exchanger NHE3. Lipid rafts (LR) modulate transport activity and are involved in phosphatidylinositol 3-kinase (PI3-kinase)-dependent trafficking of NHE3. Although DRA and NHE3 interact via PDZ adaptor proteins of the NHERF family, the role of LR and PDZ proteins in the regulation of DRA is unknown. We examined the association of DRA with LR using the nonionic detergent Triton X-100. DRA cofractionated with LR independently of its PDZ binding motif. Furthermore, DRA interacts with PDZK1, E3KARP, and IKEPP in LR, although their localization within lipid rafts is independent of DRA. Disruption of LR integrity resulted in the disappearance of DRA from LR, in a decrease of its surface expression and in a reduction of its activity. In HEK cells the inhibition of DRA by LR disruption was entirely dependent on the presence of the PDZ interaction motif. In addition, in Caco-2/BBE cells the inhibition by LR disruption was more pronounced in wild-type DRA than in mutated DRA (DRA-ETKFminus; lacking the PDZ binding motif)-expressing cells. Inhibition of PI3-kinase decreased the activity and the cell surface expression of wild-type DRA but not of DRA-ETKFminus; the partitioning into LR was unaffected. Furthermore, simultaneous inhibition of PI3-kinase and disruption of LR did not further decrease DRA activity and cell surface expression compared with LR disruption only. These results suggest that the activity of DRA depends on its LR association, on its PDZ interaction, and on PI3-kinase activity.

Cl/HCO₃ exchange; PDZK1; E3KARP; NHERF; IKEPP

ELECTRONEUTRAL NaCl absorption in the ileum and proximal colon is a major regulator of total body volume and electrolyte homeostasis. Such absorption is mediated by the integrated actions of the Na/H exchanger NHE3 (SLC9A3) and the Cl/HCO₃ exchanger downregulated in adenoma (DRA; SLC26A3). Proof for the importance of these two transporters comes from the respective knockout mice (40, 41), which suffer from chronic diarrhea, as well as the rare human disease congenital chloride diarrhea, which is caused by a loss-of-function mutation of DRA (14). Much more common though is impairment of this fundamental process by various infectious or toxic agents leading to acute secretory diarrhea (9). To address these diseases it is necessary to understand the physiological

regulation of transport proteins within enterocytes as well as the responsible extra- and intracellular signal transduction pathways. With regard to the regulation and the intracellular trafficking of DRA NHE3 may serve as a paradigm, since the functions of NHE3 and DRA appear to be regulated in parallel (21, 23).

Lipid rafts are sphingolipid- and cholesterol-rich membrane microdomains, which have been operationally defined based on their detergent insolubility and requirement of cholesterol for their physicochemical and functional integrity (4, 36). Lipid rafts were initially linked to caveolae and endocytosis but a more detailed picture has emerged, where complexes consisting of various sets of signal, adaptor and membrane proteins are temporarily gathered in lipid rafts. Based on functional data these complexes are involved in cellular processes that include membrane sorting and recycling, protein trafficking (10, 12, 15), and cell signaling (35, 43).

A subset of transport proteins are localized within lipid rafts and these have been implicated in their activity, trafficking and membrane retention as well as their regulation. For instance, disruption of raft integrity leads to decreased transport activity of NHE3 (32), the kidney-specific sodium potassium chloride cotransporter (NKCC2) (47), the serotonin transporter (30), and the calcium ATPase (PMCA) (18). At least for NHE3 the situation is complex in that its lipid raft localization is necessary not only for its normal activity but also for its basal and stimulated trafficking (27). Lipid rafts are involved in phosphatidylinositol-3 (PI3)-kinase-dependent exocytosis of NHE3 as well as in its basal endocytosis (32).

Both DRA and NHE3 possess PDZ binding motifs, which allow an interaction with members of the NHERF family of PDZ adaptor proteins (23). PDZ domain adaptor proteins have been named after the first three proteins in which they were discovered: PSD95, ZO1, and disc large. The four members of the NHERF family of PDZ proteins, NHERF, E3KARP, PDZK1 and IKEPP, as well as Shank2 and CAL, appear to play important roles for the regulation of intestinal ion transport (23). Several PDZ adaptor proteins also associate with membrane rafts. The postsynaptic density protein-95 (PSD95) directly associates with membrane rafts via covalently attached palmitoyl groups (7). Thereby it modulates the cell surface expression in lipid rafts of the voltage-gated potassium channel (Kv 1.4) (49), of the acid-sensing ion channel 3 (ASIC3) (8), and of the neuregulin receptor, ErbB4 (29). In T lymphocytes, NHERF links lipid rafts to the cytoskeleton by binding to both the lipid raft protein Cbp (COOH-terminal SRC kinase-associated membrane adaptor protein) and the actin-binding protein ezrin. This complex formation allows targeting of protein kinase A type I to lipid rafts (17, 38).

Address for reprint requests and other correspondence: G. Lamprecht, 1st Medical Dept., Univ. of Tübingen, Otfried-Müller-Str. 10, 72076 Tübingen, Germany (e-mail: hans-georg.lamprecht@uni-tuebingen.de).

Although the role of the NHERF family of adaptor proteins for the regulation, targeting, and trafficking of NHE3 and CFTR has been studied extensively, there is currently no general picture emerging (23). With regard to NHE3, DRA, and their common function for intestinal NaCl absorption the potential interplay of their raft association and their PDZ interaction has not been studied. To this end DRA has the advantage that a mutant, which lacks the PDZ interaction motif (DRA-ETK^{Fminus}), can be expressed and is functionally active (24).

Thus we tested the hypothesis that DRA is localized in lipid rafts and addressed the functional role of the PDZ interaction of DRA. Moreover, we analyzed whether lipid rafts are involved in PI3-kinase-dependent insertion of DRA into the plasma membrane.

METHODS

Materials. Nigericin, methyl- β -cyclodextrin (MCD), and Triton X-100 were from Sigma-Aldrich (Steinheim, Germany). BCECF-AM, LY294002, and the lipid raft labeling kit (Vybrant Alexa Fluor 594) were from Invitrogen (Paisley, Scotland). Sulfo-NHS-SS-biotin, NeutrAvidin agarose, and protein A-Sepharose were from Pierce (Rockford, IL). Complete protease inhibitor mixture was from Roche Applied Science (Mannheim, Germany). The monoclonal antibody against enhanced green fluorescent protein (EGFP) was from Clontech (Mountain View, CA). The monoclonal antibodies against flotillin, Rab5 and Akt were from BD Transduction (Franklin Lakes, NJ). The polyclonal antibodies against phosphorylated Akt (threonine-308-P and serine-473-P) were from Cell Signaling Technology (Danvers, MA). Anti-mouse secondary antibody and Anti-rabbit secondary antibody were from Dianova (Hamburg, Germany). FluorSave Reagent was from Merck (Darmstadt, Germany).

Cell lines. HEK293 cells stably transfected with EGFP-tagged DRA (HEK/EGFP-DRA) or EGFP-tagged DRA-ETK^{Fminus} (HEK/EGFP-DRA-ETK^{Fminus}); a DRA construct that lacks the COOH-terminal PDZ interaction motif (glutamate-threonine-lysine-phenylalanine, ETKF), were used as described previously (20). Caco-2/BBE cells expressing the Tet-Off system stably transfected with EGFP-DRA and EGFP-DRA-ETK^{Fminus} were used as described previously (24). They were routinely kept in the presence of 20 ng/ml doxycycline. Only for functional studies the expression of the DRA constructs was induced by growth in the absence of doxycycline and the cells were used 10 days after reaching confluence.

Expression constructs. EGFP-PDZK1 was used as described previously (24). Human NHERF (also known as EBP50) was amplified from the Imagenes clone IRAKp961A113 using *pfu* and primers that incorporate a *Bam*HI and a *Xho*I site (CCTTAGGGATCCATGAGCGCGGACG and GGCTCGAGGGCGCTCAGAGGTTGC). The PCR product was cloned into pCR-II-blunt TOPO (Invitrogen), sequenced and shuttled into pEGFP-C1 (Clontech) by using *Bam*HI and *Xba*I (in this case originating from the pCR-II-blunt vector backbone), resulting in pEGFP-C1/NHERF. E3KARP was reamplified by using *pfu* from pBS/E3KARP (50) using primers that introduce a *Bam*HI and a *Sal*I site (CGGCTTTTAGGATCCATGGCCGC and GCAGGAGTCGACTCAGAAGTTGCTGAA). The PCR product was cloned into pCR-II-blunt TOPO (Invitrogen), sequenced and shuttled into pEGFP-C1 (Clontech) using *Bam*HI and *Xba*I (in this case originating from the pCR-II-blunt vector backbone) resulting in pEGFP-C1/E3KARP. The coding sequence of IKEPP was amplified from the Imagenes clone IRAKp961G0550Q using *pfu* and primers that incorporate a *Hind*III and a *Xba*I site (GAAGCTTCTATGAGAAAGCCGCAGATC and TCTGTATCTAGAAGGGGTGCTTACAGTAG). The PCR product was cloned into pCR-II-blunt TOPO, sequenced and shuttled into pEGFP-C1 (Clontech) using *Hind*III and *Xba*I resulting in pEGFP-C1/IKEPP.

Cell transfection. Subconfluent (~70% confluence) HEK/EGFP-DRA or HEK/EGFP-DRA-ETK^{Fminus} cells were transiently transfected in tissue culture flasks (25 cm²) using 10 μ g expression construct of the PDZ adaptor proteins and 20 μ l Lipofectamine 2000 according to the recommendations of the manufacturer (Invitrogen). The cells were used 24 h after transfection.

Sucrose flotation gradient. Confluent monolayers in tissue culture flask (50 cm²) were washed twice with ice-cold PBS and lysed in 2 ml TNE buffer (25 mM Tris-HCl pH 7.5, 150 mM NaCl, 5 mM EDTA) containing protease inhibitor cocktail and 1% Triton X-100 (3, 37). The cells were scraped and homogenized with 10 strokes in a Dounce homogenizer. 2 ml of this lysate was mixed with an equal volume of 80% (wt/vol) sucrose in TNE buffer with protease inhibitor, transferred into a ultracentrifuge tube, and overlaid with 4 ml of 30% (wt/vol) sucrose and finally with 5% (wt/vol) sucrose (both in TNE buffer with protease inhibitor). Centrifugation was done in a Beckman SW41Ti rotor at 170,000 *g* for 19 h at 4°C. Twelve fractions were collected from the top of the gradient. In these fractions proteins were precipitated with trichloroacetic acid (TCA), size separated by 8.5% SDS-PAGE, and transferred onto nitrocellulose membranes.

MCD treatment. For cholesterol depletion 10 days confluent monolayers of Caco-2/BBE cells or 2 days confluent monolayers of HEK cells were treated with 20 mM or 1 mM MCD, respectively, in DMEM plus 0.2% BSA at 37°C for 60 min as indicated. The cells

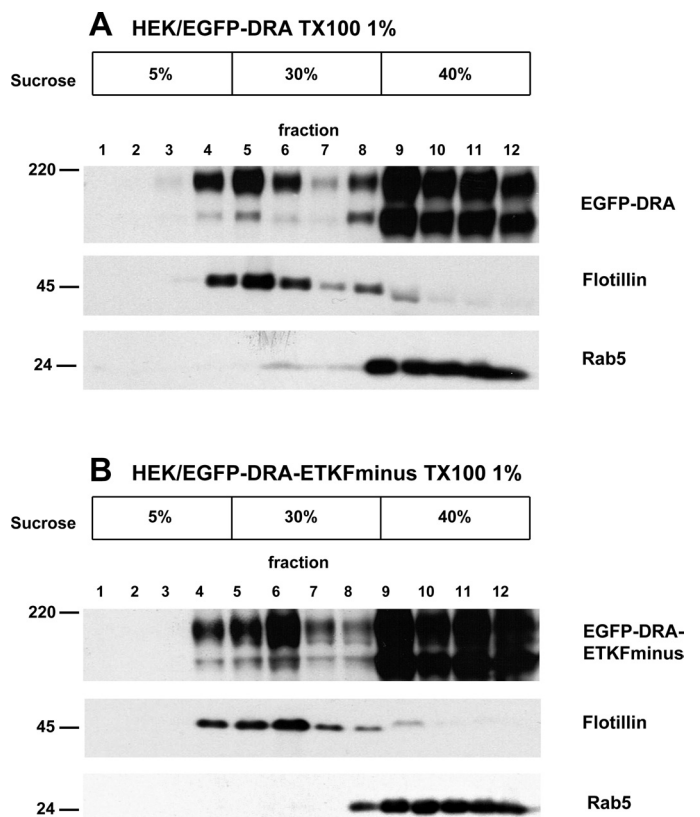


Fig. 1. Association of downregulated in adenoma (DRA) and DRA-ETK^{Fminus} with lipid rafts in stably transfected HEK cells. HEK/EGFP-DRA (A) and HEK/EGFP-DRA-ETK^{Fminus} cells (B) were lysed at 4°C using 1% Triton X-100. The lysates were subjected to sucrose density centrifugation. As a raft marker flotillin was detected in the low-density fractions 3-6 and as a nonraft marker rab5 was detected in the high-density fractions. Both EGFP-DRA and EGFP-DRA-ETK^{Fminus} were consistently detected in both low-density (lipid raft) as well as high-density (nonraft) fractions, suggesting that DRA is partially localized within lipid rafts independently of its interaction with PDZ adaptor proteins. Representative data of 5 experiments. EGFP, enhanced green fluorescent protein.

were then used for functional studies or to isolate lipid rafts by sucrose flotation gradient. In HEK cells 1 mM MCD induced a complete shift of DRA and DRA-ETKFminus from low-density to high-density fractions (data not shown), and HEK cells did not tolerate higher concentrations of MCD.

Fluorescence microscopy. Lipid rafts were labeled with cholera toxin subunit B (CT-B) using Vybrant Alexa Fluor 594 lipid raft labeling kit according to the manufacturer's protocol. Briefly, HEK/EGFP-DRA and HEK/EGFP-DRA-ETKFminus cells were grown for 3 days on coverslips. Cells were washed three times with ice-cold PBS and labeled with CT-B conjugated with Alexa Fluor 594 for 10 min at 4°C. Cells were washed three times with ice-cold PBS, and the CT-B-labeled lipid rafts clustered with anti-CT-B antibody for 10 min at 4°C. After several washings cells were fixed for 15 min with 4% formaldehyde, washed again with PBS and mounted with FluorSave

Reagent. Coverslips were examined with a Zeiss LSM510 confocal fluorescence microscope for lipid rafts (red Alexa 594 fluorescence) and DRA (green EGFP autofluorescence).

DRA activity. DRA activity was assessed as changes in the intracellular pH (pH_i) upon removal and readdition of extracellular chloride as previously described (20, 24). The pH_i traces were analyzed as described previously (25). This nonlinear curve-fitting algorithm allows the calculation of the initial slope after the change of the buffer solutions as well as the estimation of the maximal pH_i change from baseline.

Coimmunoprecipitation. Native HEK cells and HEK cells stably expressing EGFP-DRA or EGFP-DRA-ETKFminus were transiently transfected with each of the PDZ adaptor proteins of the NHERF family as an EGFP fusion protein (as described under *Cell transfection*). At 24 h after transfection the cells were used for lipid raft

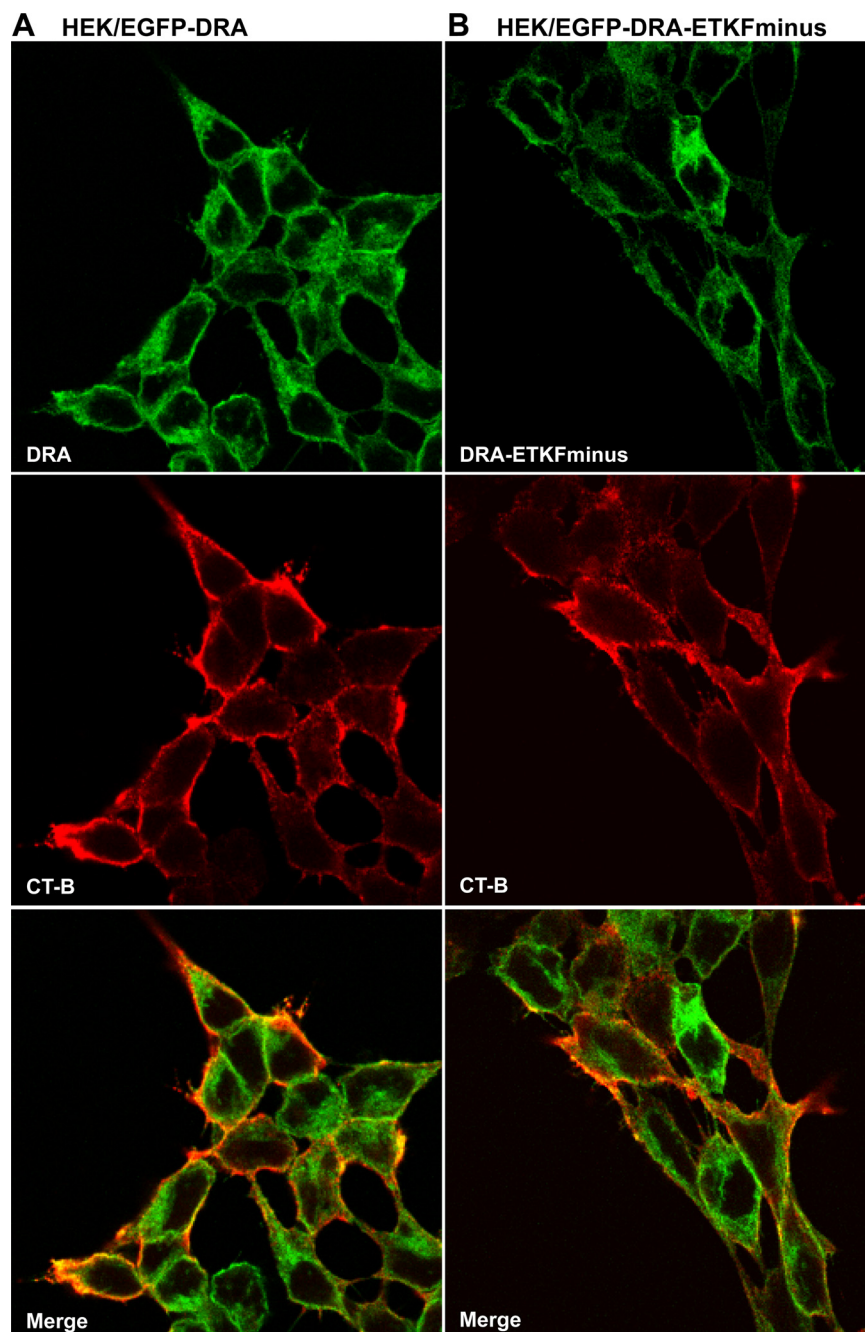


Fig. 2. DRA and DRA-ETKFminus colocalize with GM1 in stably transfected HEK cells. In HEK/EGFP-DRA (A) and HEK/EGFP-DRA-ETKFminus cells (B) the raft ganglioside GM1 was labeled with cholera toxin subunit B (CT-B) conjugated with Alexa Fluor 594. A: wild-type DRA and GM1 are partially colocalized at the cell surface. B: similarly, the DRA mutant (DRA-ETKFminus) also partially colocalized with GM1 at the cell surface.

fractionation (as described under *Sucrose flotation gradient*). Subsequently, the low-density fractions (*fractions 3-5*) were pooled (lipid raft pool). One half of this pool was used for TCA precipitation and the other half to immunoprecipitate DRA and to test for the coimmunoprecipitation of the PDZ adaptor proteins. To immunoprecipitate DRA the lipid raft pool was incubated with a DRA-specific rabbit antiserum (22) for 3 h at 4°C. After incubation the immune complexes were precipitated with protein A-Sepharose. After centrifugation the Sepharose beads were washed three times with PBS and bound immune complexes were eluted in SDS sample buffer. The eluted proteins were separated on 8.5% SDS-PAGE.

SDS-PAGE, Western blotting and immunodetection. TCA precipitated proteins were dissolved in SDS sample buffer, mixed with a 1/10 volume of 20% (wt/vol) iodoacetamide, and incubated for 15 min in the dark. (This resulted in better Western blot exposures compared with the conventional heating to 95°C for 3 min.) Equal volumes of each fraction of the sucrose flotation gradient were separated on 8.5% PAGE and blotted onto nitrocellulose. Membranes were blocked with 5% skimmed milk in TBS-T (20 mM Tris-base 7.5 pH, 150 mM NaCl, 0.1% Tween 20) and subsequently incubated with an anti-EGFP monoclonal antibody (1:500), an anti-flotillin-1 monoclonal antibody (1:250), or an anti-rab5 monoclonal antibody (1:1,000) followed by incubation with horseradish peroxidase-conjugated goat anti-mouse IgG (1:5,000). The immunoblots were developed by use of chemiluminescence (ECL+plus, Pierce).

Akt phosphorylation. The effect of LY294002 on PI3-kinase was tested by determining the phosphorylation status of the PI3-kinase substrate Akt. HEK/EGFP-DRA or HEK/EGFP-DRA-ETKFminus cells were incubated with 50 μ M LY294002 for 30 min at 37°C and then lysed in 1 ml of 100 mM NaCl, 50 mM NaF, 20 mM Tris, 1% Triton X-100, and 125 μ l/ml complete protease inhibitor mixture by passing them 15 times through a 22-gauge needle. Equal amounts of protein were separated by SDS-PAGE and blotted. Akt, Akt-Thr-308-P, and Akt-Ser-473-P were detected using anti-Akt monoclonal antibody (1:1,000), anti-Akt-Thr-308-P polyclonal antibody (1:1,000), and anti-Akt-Ser-473-P polyclonal antibody (1:1,000).

Cell surface biotinylation. Confluent monolayers of transfected HEK cells were washed twice with ice-cold PBS containing calcium

and magnesium and once with borate buffer (154 mM NaCl, 10 mM boric acid, 7.2 mM KCl, 1.8 mM CaCl₂) and were incubated twice with biotinylation buffer (1 mg/ml sulfo-NHS-SS-biotin in borate buffer) at 4°C for 30 min. To remove the unbound biotin, the cells were washed with ice-cold quenching buffer (25 mM Tris-base, 120 mM NaCl, 1.8 mM CaCl₂) and incubated with quenching buffer for 5 min at 4°C. After two washes with ice-cold PBS the cells were lysed in 1 ml of 100 mM NaCl, 50 mM NaF, 20 mM Tris-base, 1% Triton X-100, and 125 μ l/ml complete protease inhibitor mixture by passing them 15 times through a 22-gauge needle. The lysate was cleared by spinning for 10 min at 10,000 g and was then tumbled with 200 μ l NeutrAvidin-agarose beads overnight at 4°C. After multiple washing the biotinylated proteins were eluted from the beads by use of sample buffer, separated by SDS-PAGE, and blotted onto nitrocellulose. EGFP-DRA and EGFP-DRA-ETKFminus were detected as described above. Bands were quantified by using ImageMaster 1D, version 3.0 (Amersham Biosciences), with manual background subtraction. Relative changes of DRA surface expression were analyzed by normalization of the band intensity of biotinylated EGFP-DRA to the band intensity of total EGFP-DRA in the lysate.

Statistical analysis. All statistical calculations were done using Jump 5.1 (SAS Institute, Cary, NC). All data are presented as means \pm SD. ANOVA and *t*-tests were applied when appropriate.

RESULTS

DRA is associated with lipid rafts. Lipid rafts have been defined operationally as detergent-resistant membranes that float at the 5%/30% interface in sucrose gradients (4). To investigate whether DRA is present in lipid rafts, we lysed HEK cells stably expressing EGFP-DRA or EGFP-DRA-ETKFminus (the DRA mutant, which lacks the COOH-terminal PDZ interaction motif) in 1% Triton X-100 (3, 37) and separated fractions by density using a discontinuous sucrose gradient. We used flotillin as a marker for lipid rafts because HEK cells do not express caveolin (39). As expected, flotillin (48 kDa) was detected in the low-density *fractions 3, 4, 5,* and

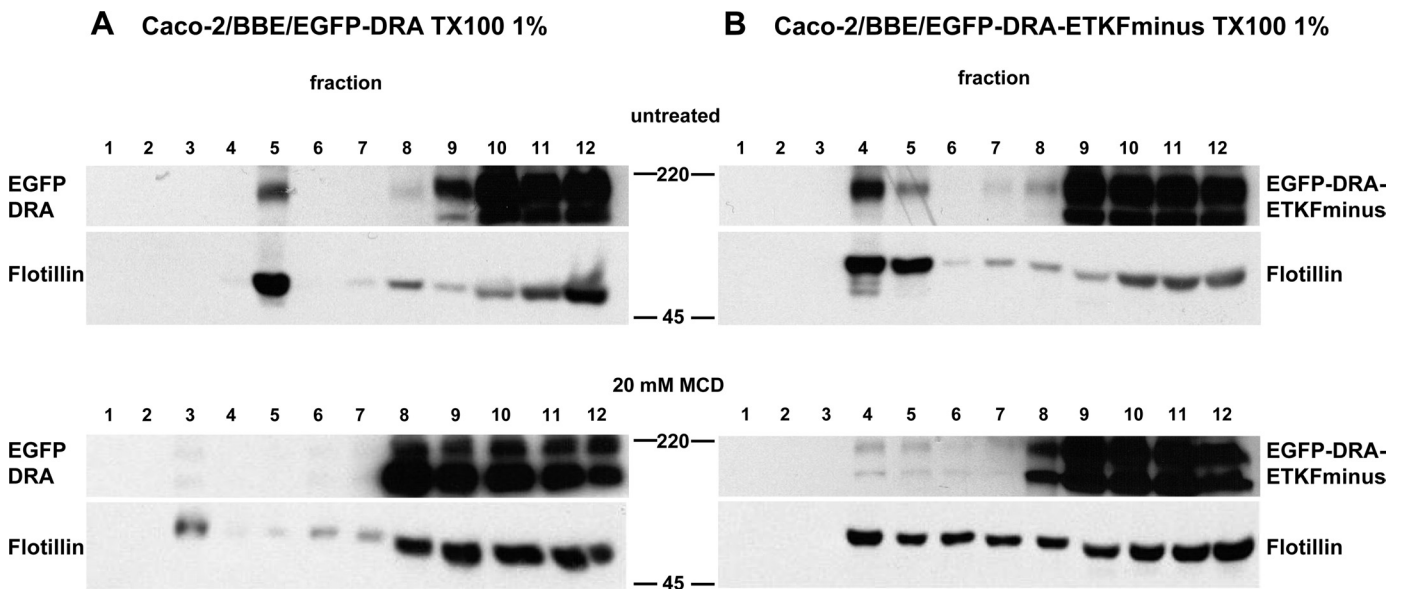
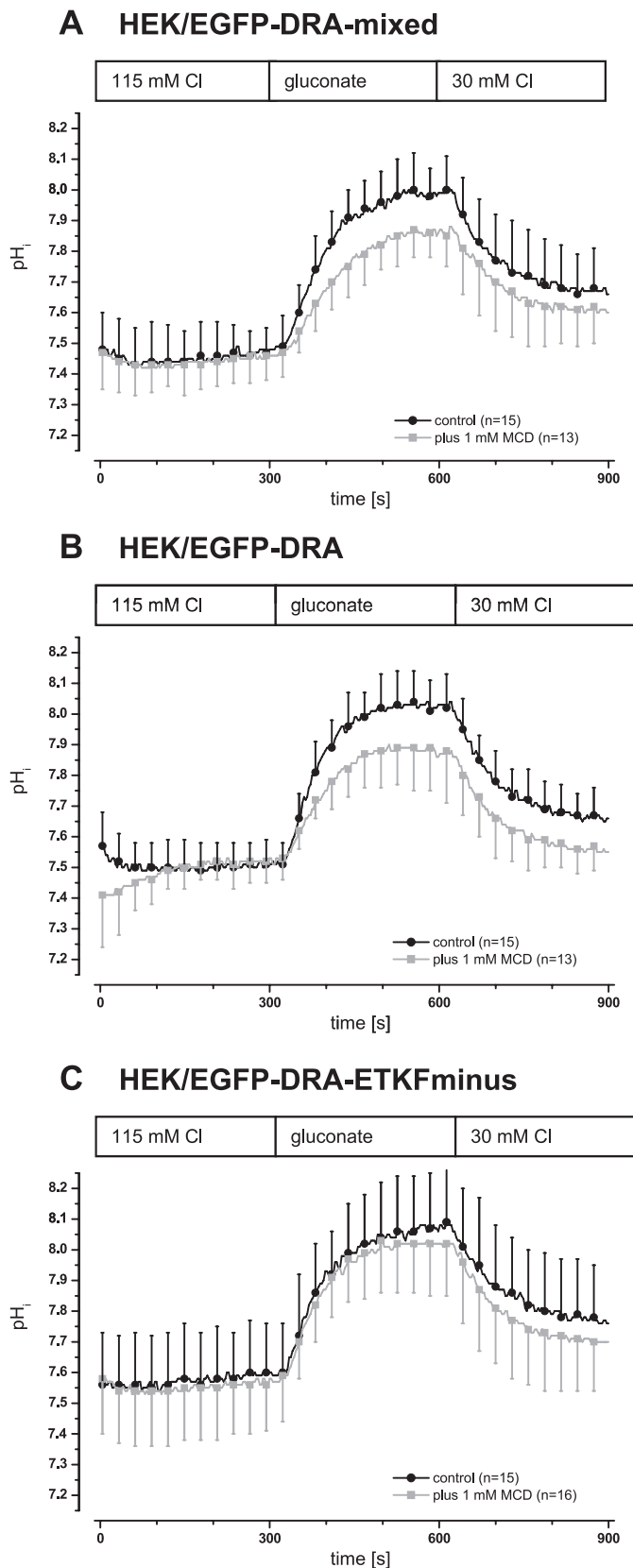


Fig. 3. The lipid raft association of DRA and DRA-ETKFminus is sensitive to cholesterol depletion. Caco-2/BBE/EGFP-DRA (A) and Caco-2/BBE/EGFP-DRA-ETKFminus (B) cells were lysed with 1% Triton X-100 and subjected to density gradient centrifugation. *Top*: in untreated cells EGFP-DRA and EGFP-DRA-ETKFminus float to low-density lipid raft fractions as evidenced by their cosegregation with the raft marker flotillin. *Bottom*: treatment with 20 mM methyl- β -cyclodextrin (MCD) at 37°C for 60 min completely shifted both EGFP-DRA and EGFP-DRA-ETKFminus out of the low-density raft fractions, whereas flotillin was only incompletely shifted. Representative data of 4 experiments.



6 with a peak at the interface between 5 and 30% sucrose (Fig. 1). These data are consistent with lipid rafts floating in low-density fractions, whereas most other membranes are solubilized by these detergents and will thus be detected in the high-density fractions. As a nonraft marker we analyzed the distribution of the GTPase rab5 (5). As expected, rab5 was exclusively found in the high-density fractions, demonstrating the ability of the gradient to isolate raft from nonraft fractions with high specificity.

An EGFP-specific monoclonal antibody detected EGFP-DRA (Fig. 1A) and EGFP-DRA-ETKFminus (Fig. 1B) as bands of 180 and 145 kDa. Both proteins were predominantly present in the high-density fractions but a small amount of both reproducibly appeared in the low-density, flotillin-containing fractions. Minor differences in the distribution of DRA or DRA-ETKFminus are due to the fractionation of the gradients in the individual experiment displayed and were not a reproducible phenomenon (e.g., fractions 5 and 6 in Fig. 1, A and B). These data indicate that DRA is present in lipid raft and that this association is independent of the PDZ interaction of DRA.

To confirm the localization of DRA and DRA-ETKFminus in lipid rafts, we labeled the raft protein GM1 with CT-B (conjugated with Alexa Fluor 594) (11) and determined the colocalization of EGFP-DRA and EGFP-DRA-ETKFminus with GM1 by confocal fluorescence microscopy. Both EGFP-DRA and EGFP-DRA-ETKFminus partially colocalized with GM1 at the cell surface (Fig. 2).

Depletion of cholesterol reduces the pool of DRA in lipid rafts. Cholesterol is essential for the integrity of lipid rafts (4). MCD binds cholesterol (16), thereby depleting membrane cholesterol and disrupting lipid rafts. This causes raft-associated proteins to shift from low-density to high-density fractions. The effect of raft disruption on partitioning of EGFP-DRA and EGFP-DRA-ETKFminus was therefore assessed.

MCD treatment completely shifted EGFP-DRA and EGFP-DRA-ETKFminus bands from the low-density to the high-density fractions (Fig. 3). Flotillin was also shifted to high-density fractions by MCD treatment (Fig. 3), but this shift was incomplete. Further reductions of cellular cholesterol induced by extended incubation of the cells with lovastatin were necessary to shift the majority of flotillin to high-density fractions (data not shown). These data, obtained in a well-differentiated intestinal cell line, further substantiate the partial localization of DRA in lipid rafts, which is independent of its PDZ interaction in both transfected HEK and Caco-2/BBE cells.

Fig. 4. In transfected HEK cells DRA is inhibited by disruption of raft integrity. DRA activity was assayed as intracellular alkalization upon removal of chloride and reacidification upon readdition of chloride. Raft integrity was disrupted by incubation of the cells in 1 mM MCD at 37°C for 60 min prior to the experiment. *A*: in a mixed population (i.e., nonclonal) of HEK/EGFP-DRA cells DRA activity was inhibited involving both the maximal intracellular pH (pH_i) change as well as the initial slope (maximal ΔpH_i ; 0.60 ± 0.09 vs. 0.51 ± 0.06 , -16% , $P < 0.05$; initial slope 0.47 ± 0.15 pH/min vs. 0.29 ± 0.10 , -38% , $P < 0.05$). *B*: this finding was corroborated in clonal HEK/EGFP-DRA cells (maximal ΔpH_i ; 0.62 ± 0.07 vs. 0.46 ± 0.21 , -28% , $P < 0.05$; initial slope 0.61 ± 0.16 pH/min vs. 0.37 ± 0.15 , -39% , $P < 0.05$). *C*: in clonal HEK/EGFP-DRA-ETKFminus cells (the DRA mutant that lacks the PDZ interaction motif) there was no inhibition by MCD (maximal ΔpH_i ; 0.58 ± 0.09 vs. 0.53 ± 0.04 , -4% , $P > 0.05$; initial slope 0.47 ± 0.18 pH/min vs. 0.50 ± 0.16 , $+5\%$, $P > 0.05$).

In HEK cells, disruption of lipid raft integrity inhibits DRA, a process that involves the PDZ interaction of DRA. We next asked whether the partial localization of DRA in lipid rafts has an influence on DRA activity. DRA activity was assayed and analyzed as changes in the pH_i upon removal and readdition of

extracellular chloride as previously described (20, 25). This approach results in calculated absolute values for the maximal pH_i change as well as for the initial slope of the pH_i trace after the change of the buffer solutions. These absolute values were then analyzed to assess the effect of MCD.

Wild-type DRA expressed in a mixed population of stably transfected HEK cells was inhibited by MCD treatment (Fig. 4A), resulting in both reduced maximal pH_i change and altered initial slope (maximal ΔpH_i 0.60 ± 0.09 vs. 0.51 ± 0.06 , -16% , $P < 0.05$; initial slope 0.47 ± 0.15 pH/min vs. 0.29 ± 0.10 , -38% , $P < 0.05$). This finding was corroborated in a HEK cell clone expressing wild-type DRA (Fig. 4B, maximal ΔpH_i 0.62 ± 0.07 vs. 0.46 ± 0.21 , -28% , $P < 0.05$; initial slope 0.61 ± 0.16 pH/min vs. 0.37 ± 0.15 , -39% , $P < 0.05$). In contrast, MCD did not affect the activity of EGFP-DRA-ETKfminus, which lacks the PDZ interaction motif (Fig. 4C, maximal ΔpH_i 0.58 ± 0.09 vs. 0.53 ± 0.04 , -4% , $P > 0.05$; initial slope 0.47 ± 0.18 pH/min vs. 0.50 ± 0.16 , $+5\%$, $P > 0.05$). Together these data suggest that in transfected HEK cells part of the activity of DRA is dependent on its localization in lipid rafts and that this part is dependent on the interaction of DRA with one or several PDZ adaptor proteins.

Disruption of lipid raft integrity inhibits DRA activity in Caco-2/BBE cells. The effect of MCD on DRA-mediated Cl/HCO_3 exchange was also assessed in well-differentiated intestinal epithelial Caco-2/BBE cells.

In EGFP-DRA expressing Caco-2/BBE cells, the maximal pH_i change after removal of chloride was reduced by 32% (maximal ΔpH_i 0.42 ± 0.09 vs. 0.28 ± 0.08 , $P < 0.05$) and the initial slope was reduced by 37% (0.27 ± 0.13 pH/min vs. 0.17 ± 0.08 , $P < 0.05$) after MCD treatment (Fig. 5A). Although the activity of EGFP-DRA-ETKfminus was also reduced by MCD (Fig. 5B) in Caco-2/BBE cells (maximal ΔpH_i 0.50 ± 0.07 vs. 0.41 ± 0.09 , -17% , $P < 0.05$; initial slope 0.45 ± 0.09 pH/min vs. 0.39 ± 0.10 , -13% , but $P > 0.05$), the magnitude of inhibition was less than wild-type DRA. After preincubation with MCD the baseline pH_i of untransfected and transfected Caco-2/BBE cells was lower than that of untreated cells. But this effect was statistically not different between the three cell lines (Fig. 5, A, B, and C), suggesting that it was due to an effect of MCD on a mechanism other than DRA that affects the baseline pH_i .

The more pronounced inhibition by MCD of wild-type DRA, relative to DRA-ETKfminus, suggests that DRA activity in intestinal epithelial cells is partially dependent on its raft localization. Moreover, the raft-dependent activity of DRA has

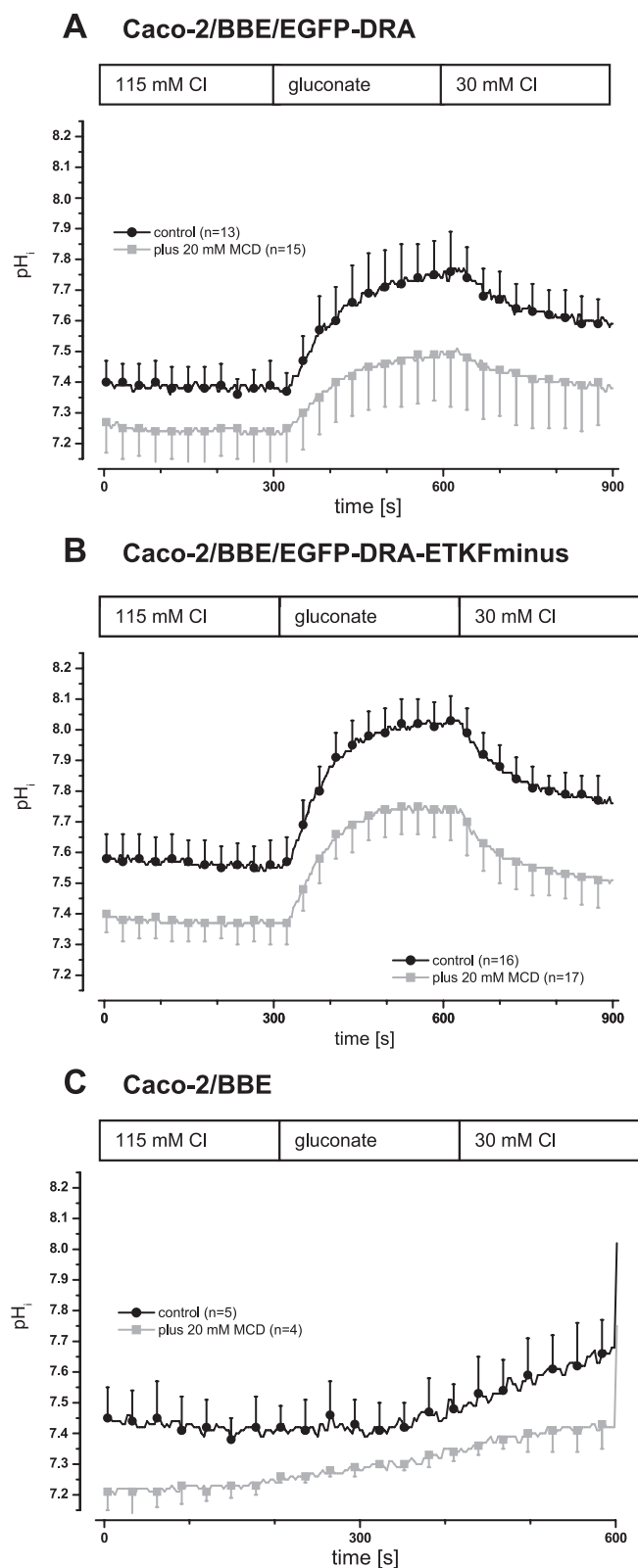


Fig. 5. In transfected Caco-2/BBE cells DRA is inhibited by disruption of lipid raft integrity. DRA activity was assayed as intracellular alkalization upon chloride removal and reacidification upon readdition of chloride. Raft integrity was disrupted by incubation of the cells with 20 mM MCD at 37°C for 60 min prior to the experiment. A: in clonal Caco-2/BBE/EGFP-DRA cells both the maximal ΔpH_i and the initial slope were reduced by 32 and 37%, respectively (maximal ΔpH_i 0.42 ± 0.09 vs. 0.28 ± 0.08 , $P < 0.05$; initial slope 0.27 ± 0.13 pH/min vs. 0.17 ± 0.08 , $P < 0.05$). B: in clonal Caco-2/BBE/DRA-ETKfminus cells this inhibition was less pronounced (maximal ΔpH_i 0.50 ± 0.07 vs. 0.41 ± 0.09 , -17% , $P < 0.05$; initial slope 0.45 ± 0.09 pH/min vs. 0.39 ± 0.10 , -13% , but $P > 0.05$). C: preincubation with 20 mM MCD of untransfected Caco-2/BBE cells reduced the baseline pH_i (-0.14 pH units, $P < 0.05$) as it did in the 2 transfected cell lines (-0.14 pH units in Caco-2/BBE/EGFP-DRA, $P < 0.05$ and -0.19 pH units, $P < 0.05$ in Caco-2/BBE/EGFP-DRA-ETKfminus cells).

two components, one which is dependent and another which is independent of its PDZ interactions.

Cell surface expression of DRA is reduced by MCD. The inhibitory effect of raft disruption could be secondary to decreased DRA expression at the cell surface. The fraction of DRA at the cell surface was determined by biotinylation of control and MCD-treated cells. In control cells $21.7 \pm 4.8\%$ of total DRA was detected at the surface, whereas only $16.1 \pm 2.4\%$, a 25% reduction ($P < 0.05$), was at the surface of cells treated with MCD (Fig. 6A). In contrast, MCD treatment of HEK cells expressing the mutated DRA (EGFP-DRA-ETK-Fminus) did not result in a reduction of the cell surface expression (control $24.2 \pm 3.2\%$ and after MCD treatment $23.3 \pm 5.0\%$ cell surface expression, $P > 0.05$) (Fig. 6B). These data indicate that the effect of disruption of raft integrity results in a reduction of cell surface expression of DRA, which requires an interaction with one or several PDZ adaptor proteins.

Inhibition of PI3-kinase decreases activity and cell surface expression of DRA. Even under basal conditions NHE3 traffics between recycling endosomes and the cell surface in a PI3-kinase-regulated, lipid raft-dependent manner (32). Given the parallel functions of NHE3 and DRA in absorption, we asked whether membrane insertion of DRA occurs in a similar manner.

First we analyzed whether basal DRA activity was influenced by inhibition of PI3-kinase and whether this was dependent on the PDZ interaction of DRA. HEK/EGFP-DRA and HEK/EGFP-ETK-Fminus cells were incubated with LY294002, an inhibitor of PI3-kinase. This led to an inhibition of wild-type DRA (maximal ΔpH_i 0.56 ± 0.06 vs. 0.45 ± 0.04 , -19% , $P < 0.05$; initial slope 0.52 ± 0.16 pH/min vs. 0.44 ± 0.07 , -15% , $P > 0.05$) (Fig. 7A). In contrast, DRA-ETK-Fminus was not inhibited by LY294002 (maximal ΔpH_i 0.56 ± 0.07 vs. 0.57 ± 0.07 , $+2\%$, $P > 0.05$; initial slope 0.89 ± 0.19 pH/min vs. 0.86 ± 0.17 , -3% , $P > 0.05$) (Fig. 7B).

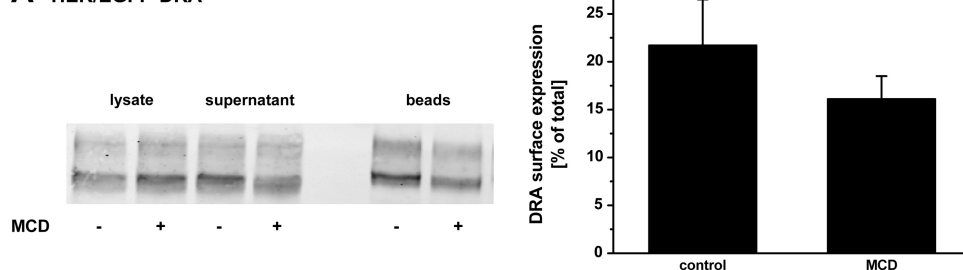
Additionally, we examined whether the inhibition of PI3-kinase also decreases the cell surface expression of DRA. Inhibition of PI3-kinase led to a reduction of the cell surface expression of wild-type DRA. In control cells $20.2 \pm 2.6\%$ of total DRA was detected at the surface, whereas only $15.9 \pm 1.2\%$, a 21% reduction ($P < 0.05$), of DRA was at the surface of cells treated with LY294002 (Fig. 8A). In contrast, the cell surface expression of DRA-ETK-Fminus was not reduced by LY294002 (control $24.7 \pm 4.4\%$ and after LY294002 treatment $27.3 \pm 5.4\%$, $P > 0.05$) (Fig. 8B).

These data suggest that basal exocytosis of DRA involves the action of PI3-kinase and is dependent on the interaction of DRA with one or several PDZ domain proteins.

PI3-kinase may either affect the presence of DRA (and DRA-ETK-Fminus) within lipid rafts or it may inhibit the insertion of intracellular vesicles into the plasma membrane. To address these possibilities, the effect of LY294002 on the distribution of DRA and DRA-ETK-Fminus in lipid raft and nonraft fractions was assessed. HEK/EGFP-DRA and HEK/EGFP-DRA-ETK-Fminus cells were treated with $50 \mu\text{M}$ LY294002 and fractionated on a sucrose gradient to separate lipid rafts from nonraft fractions. As can be seen in Fig. 9, inhibition of PI3-kinase did not abrogate the distribution of EGFP-DRA and EGFP-DRA-ETK-Fminus in lipid rafts, indicating that PI3-kinase is not responsible for raft localization of DRA. Together with the data presented in Fig. 8, these findings suggest that DRA is present in lipid rafts in an intracellular compartment before it is inserted into the plasma membrane.

To validate that LY294002 actually inhibits PI3-kinase, we assessed the phosphorylation status of the PI3-kinase substrate, Akt, in the absence and presence of LY294002. Under control conditions, both phosphorylation sites (threonine-308 and serine-473) of Akt were phosphorylated. As expected $50 \mu\text{M}$ LY294002 abrogated phosphorylation of both sites (Fig. 10).

A HEK/EGFP-DRA



B HEK/EGFP-DRA-ETK-Fminus

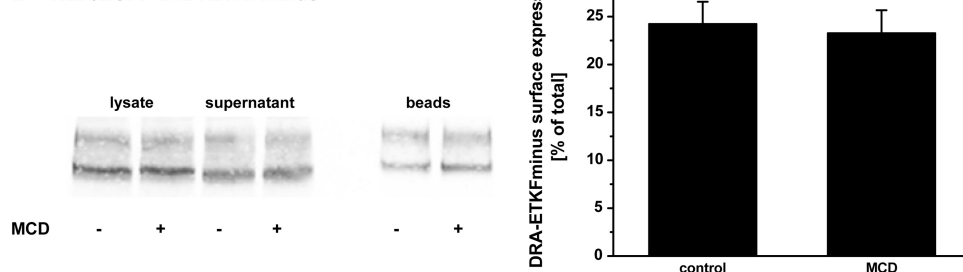


Fig. 6. Surface expression of DRA is decreased by disruption of raft integrity. HEK/EGFP-DRA (A) and HEK/EGFP-DRA-ETK-Fminus (B) cells were treated with 1 mM MCD for 60 min at 37°C . Cells were then surface-labeled with sulfo-NHS-SS-biotin at 4°C . Biotinylated proteins were retrieved by NeutrAvidin precipitation. Surface expression was calculated as the percentage of total DRA in the lysate. All experiments had a recovery (biotinylated + nonbiotinylated) of 85–115% of total DRA. *Left*: representative blots. *Right*: summaries of 3–4 experiments.

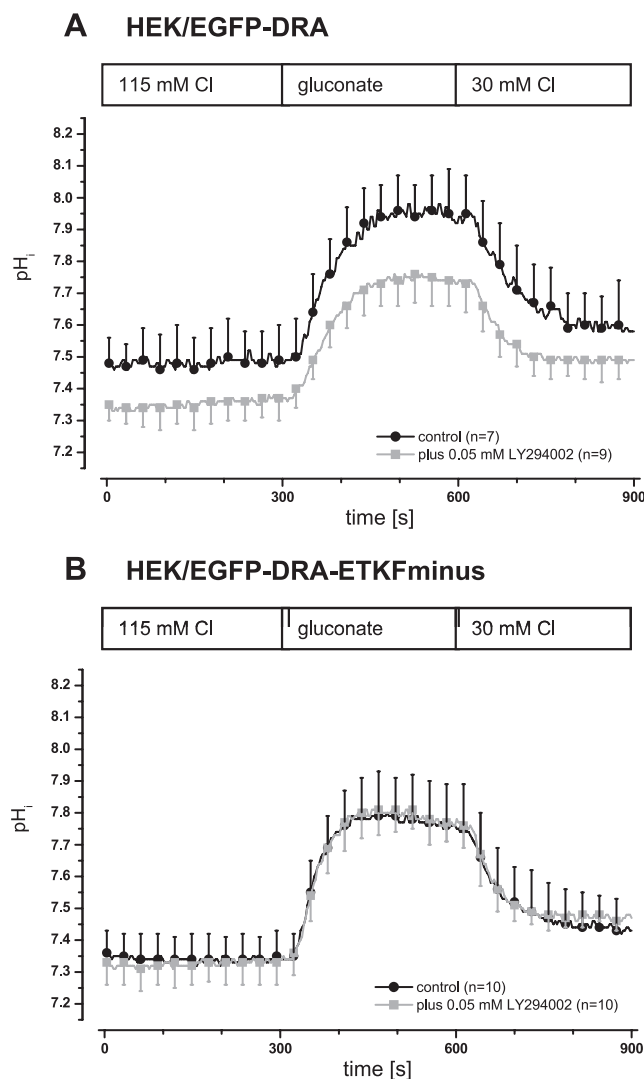


Fig. 7. DRA activity depends on PI3-kinase activity and on the PDZ interaction of DRA. In HEK/EGFP-DRA (A) and in EGFP-DRA-ETKFminus (B) cells PI3-kinase was inhibited by incubation with 50 μ M LY294002 for 30 min at 37°C prior to the functional experiment. Inhibition of PI3-kinase leads to a reduction of Cl/HCO₃ exchange only in cells expressing wild-type DRA (A) (maximal Δ pH_i 0.56 ± 0.06 vs. 0.45 ± 0.04 , -19% , $P < 0.05$; initial slope 0.52 ± 0.16 pH/min vs. 0.44 ± 0.07 , -15% , $P > 0.05$) but not in cells expressing the mutated DRA (B) (maximal Δ pH_i 0.56 ± 0.07 vs. 0.57 ± 0.07 , $+2\%$, $P > 0.05$; initial slope 0.89 ± 0.19 pH/min vs. 0.86 ± 0.17 , -3% , $P > 0.05$).

Lipid rafts are involved in basal insertion of DRA into the plasma membrane. Given that raft disruption and PI3-kinase inhibition both inhibited wild-type DRA to a similar extent (25 and 21%, respectively), we asked whether these treatments acted on the same regulatory pathway. Incubation of HEK/EGFP-DRA cells with MCD inhibited DRA by 34% (maximal Δ pH_i 0.44 ± 0.07 vs. 0.29 ± 0.07 , $P < 0.05$; initial slope 0.45 ± 0.10 pH/min vs. 0.34 ± 0.12 , -25% , $P > 0.05$), but treatment with both MCD and LY294002 did not reduce DRA activity further (maximal Δ pH_i 0.24 ± 0.07 , -45% compared with control, $P < 0.05$, but not significantly different from MCD treated cells; and initial slope 0.37 ± 0.16 pH/min, -18% , $P > 0.05$) (Fig. 11).

The data suggest that PI3-kinase and lipid rafts are situated along a common route of DRA trafficking. Functionally this indicates that lipid rafts are involved in PI3-kinase-dependent basal insertion of wild-type DRA into the plasma membrane.

PDZ adaptor proteins of the NHERF family are associated with lipid rafts. The PDZ adaptor proteins NHERF (also known as EBP50), E3KARP, PDZK1, and IKEPP interact with the PDZ binding motifs of NHE3, DRA and CFTR and may be involved in the surface expression of these transporters (23). There was no difference in the raft association of DRA compared with DRA-ETKFminus (see Figs. 1–3), suggesting that the raft association of DRA is not a consequence of its interaction with PDZ adaptor proteins. On the other hand the data shown above indicate that DRA activity and its PI3-kinase-regulated trafficking depend on the interaction with one or several PDZ adaptor proteins as well as on its lipid raft localization. As a first step to integrate these findings we tested, whether members of the NHERF family associate with lipid rafts and whether this association depends on the expression of DRA in lipid rafts.

Native HEK cells, HEK/EGFP-DRA, and HEK/EGFP-DRA-ETKFminus cells were transiently transfected with each of the PDZ adaptor proteins of the NHERF family.

EGFP-PDZK1 was detected both in the low-density and in the high-density fractions in all three cell lines (Fig. 12A). However, similar to DRA and DRA-ETKFminus, only a small amount of PDZK1 was recovered in the flotillin-containing fractions. These data suggest that PDZK1 is partially localized within rafts, but that this localization is independent of DRA, i.e., PDZK1 is not recruited by DRA to lipid rafts.

IKEPP and E3KARP followed a similar flotation pattern as PDZK1 as they were detected in both the low-density and the high-density fractions. (Fig. 12, B and C). IKEPP and E3KARP are thus also partially localized within lipid rafts, and this is again independent of their potential for interaction with DRA in rafts.

In contrast to PDZK1, IKEPP, and E3KARP, NHERF was only detected in the high-density fractions of all three cell lines (Fig. 12D). These results suggest that NHERF is not localized within lipid rafts.

DRA interacts with PDZK1, E3KARP, and IKEPP within lipid rafts. DRA and the PDZ adaptor proteins PDZK1, E3KARP, and IKEPP are partially localized within lipid rafts. However, it is unknown whether DRA interacts with these PDZ adaptor proteins within lipid rafts. To address this, we performed coimmunoprecipitation of EGFP-tagged PDZ adaptor proteins with DRA in lipid raft fractions. Expression of the respective PDZ adaptor construct and DRA in this pool was confirmed as described for Figs. 1 and 12. Furthermore, the pooled material was subjected to immunoprecipitation of DRA with a rabbit polyclonal anti-DRA antibody (22). The immunoprecipitated material was then tested for coimmunoprecipitation of the EGFP-tagged PDZ adaptor construct by using the monoclonal anti-EGFP antibody.

In Fig. 13 the results of the confirmation of the expression of EGFP-PDZ adaptor construct and EGFP-DRA or EGFP-DRA-ETKFminus in the lipid raft pool are shown on the *left* and the results of the coimmunoprecipitation are shown on the *right*. PDZK1, IKEPP, and E3KARP were each detected in the lipid raft pool, confirming the results of Fig. 12. PDZK1, IKEPP, and E3KARP were all coimmunoprecipitated with wild-type

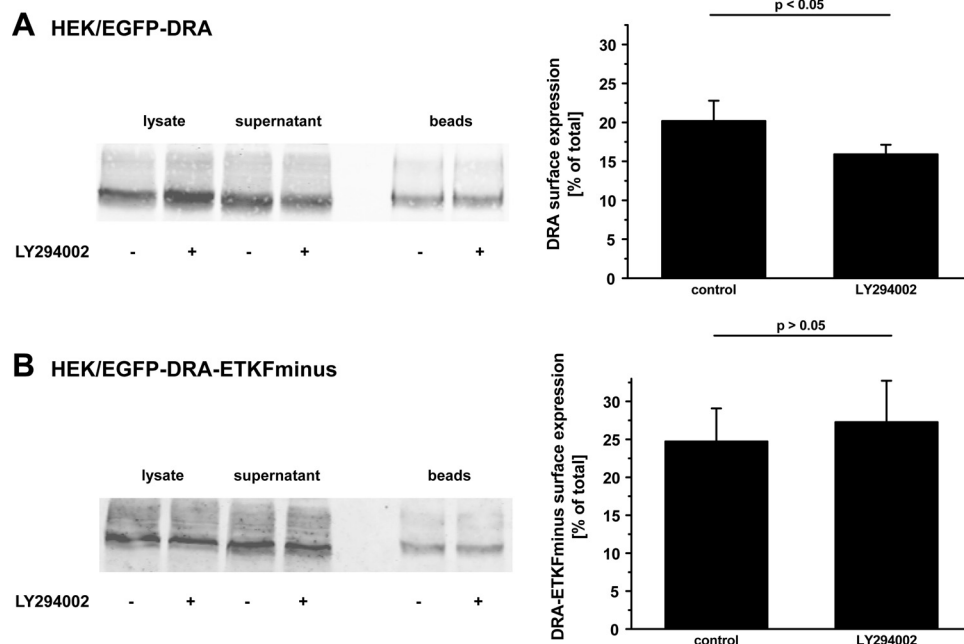


Fig. 8. Surface expression of DRA is reduced by inhibition of PI3-kinase. HEK/EGFP-DRA (A) and HEK/EGFP-DRA-ETKFminus (B) cells were treated with 50 μ M LY294002 for 30 min at 37°C. As in Fig. 6, cell surface expression was assessed by biotinylation and calculated as the percentage of total DRA. All experiments had a recovery (biotinylated + nonbiotinylated) of 85–115% of total DRA. LY294002 reduced surface expression of wild-type DRA by 21% whereas that of DRA-ETKFminus remained unchanged. *Left*: representative blots. *Right*: summaries of 3–4 experiments.

DRA in the lipid raft pool. As expected, no PDZ adaptor protein construct was coimmunoprecipitated from native HEK or from EGFP-DRA-ETKFminus-expressing cells, confirming the specificity of the coimmunoprecipitation. Taken together these data indicate that DRA and also PDZK1, IKEPP, and E3KARP are not only expressed in lipid rafts but also interact with each other in this specialized cellular compartment. Based on the band intensity the strongest interaction occurs between DRA and PDZK1. This is in agreement with unpublished data from our group showing that PDZK1 has the highest affinity to DRA.

DISCUSSION

NHE3, the functional partner of DRA in the context of intestinal NaCl absorption, is present in lipid rafts (26, 27, 32). We therefore hypothesized that DRA might also be present in lipid rafts. Both proteins interact with a common set of intracellular PDZ adaptor proteins, but the functional roles of these interactions are complex (23). Finally, the potential interplay between lipid raft association and PDZ interaction has not been studied for either NHE3 or DRA. We addressed these questions in transfected HEK and Caco-2/BBE cells expressing EGFP-tagged DRA constructs, because these systems allow us to measure DRA activity at a low background of Cl/HCO₃ exchange and because we can specifically compare wild-type DRA to DRA-ETKFminus (20, 24). In addition, in our Caco-2/BBE cells endogenous expression of DRA is too low to be detected in the lipid raft compartment. In the past our attempts to express untagged DRA have not been successful (20). Nevertheless confocal images obtained previously suggest that EGFP-DRA is expressed in the apical membrane and microvilli of Caco-2/BBE cells (24). Our present data show the following: 1) DRA is localized within lipid rafts independently of its PDZ interaction. 2) Disruption of lipid raft integrity leads to functional inhibition and decreased cell surface expression of DRA. In HEK cells the inhibition of DRA activity as well as the decreased cell surface expression are entirely dependent on

the presence of the PDZ interaction motif of DRA, and thus it involves the interaction of DRA with one or several PDZ adaptor proteins. In Caco-2/BBE cells on the other hand only part of the inhibition of DRA activity by MCD is dependent on the ability of DRA to interact with PDZ adaptor proteins. 3) Basal activity as well as basal surface expression of DRA depend on PI3-kinase activity in a way that requires the ability of DRA to interact with PDZ adaptor proteins. 4) Lipid rafts and PI3-kinase are situated along the same pathway, where DRA is present in lipid rafts before it is inserted into the plasma membrane. 5) The PDZ adaptor proteins PDZK1, IKEPP, and E3KARP are present within lipid rafts. Although these adaptor proteins are not recruited by DRA to lipid rafts, PDZK1 (and to a lesser degree or with lower affinity IKEPP and E3KARP) also interacts with DRA in lipid rafts.

The fraction of DRA (both wild-type and the mutant lacking the PDZ interaction motif) as well as that of PDZK1, E3KARP, and IKEPP within lipid rafts was relatively small. Such partial association has been observed in several other systems and with several other proteins (13, 31, 33). It may reflect that the association with lipid rafts is only transient or is specifically regulated. The isolation of lipid rafts by detergent extraction and overnight ultracentrifugation through a density gradient induces a static profile of raft associated proteins. Thus it may not detect dynamic associations (42). In addition, the distribution of protein within microdomains may increase in response to a stimulus. A similar situation has been described with several other transporters. For instance, vasopressin induces recruitment of the Na-K-Cl-cotransporter (NKCC2) to lipid rafts (47). Furthermore, the stimulation of NHE3 by epidermal growth factor is associated with an increase of the amount of NHE3 within lipid rafts (27). To this end it must be noted that the present studies were all done under basal conditions, i.e., in the absence of extracellular stimuli of DRA, but without serum starvation. Despite the relatively small amount of DRA present in lipid rafts, disruption of their integrity had a large inhibitory effect on DRA activity. Thus lipid rafts play an important

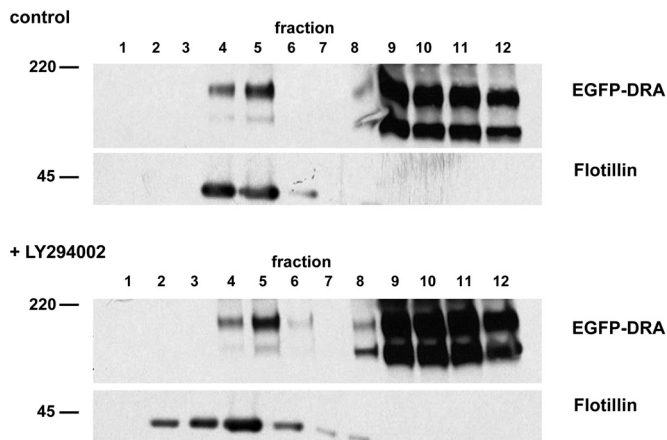
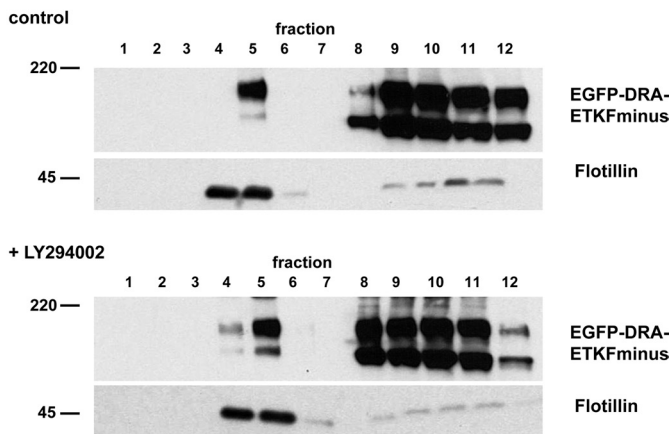
A HEK/EGFP-DRA TX100 1%**B HEK/EGFP-DRA-ETKFminus TX100 1%**

Fig. 9. Inhibition of PI3-kinase does not affect the presence of DRA in lipid rafts. HEK/EGFP-DRA (A) and HEK/EGFP-DRA-ETKFminus cells (B) were incubated with 50 μ M LY294002 and fractionated as described for Fig. 1 to separate lipid rafts from nonraft fractions. Comparison of treated with untreated cells shows no significant difference with regard to the presence of DRA or DRA-ETKFminus in lipid rafts (flotillin-positive fractions 4 and 5). Representative data of 3 experiments.

physiological role for intestinal NaCl absorption, related not only to NHE3 but also to DRA.

In HEK cells the disruption of raft integrity decreased the transport activity of wild-type DRA but not of DRA-ETKFminus. These data strongly suggest an intimate and physiologically important relationship between the lipid raft association and the PDZ interaction of DRA. This finding is also technically important because the specificity of the effect for the wild-type protein indicates that the biological effect of MCD is specific and not merely toxic. In Caco-2/BBE cells on the other hand the disruption of raft integrity reduced the activity of wild-type DRA and in addition, but to a lesser extent, also of DRA-ETKFminus. Thus in Caco-2/BBE cells the lipid raft dependent activity of DRA has two components, one that requires the interaction with one or several PDZ adaptor proteins and one that is independent of the PDZ interaction. This component is reminiscent of findings in transfected OK cells, where lipid rafts are also involved in the basal endocytosis of transfected NHE3 (32).

PI3-kinase is involved in both endo- and exocytosis (28). Inhibition of PI3-kinase mediated exocytosis results in a decreased plasma membrane fraction and thus most likely also decreased activity of a transport protein. Inhibition of endocytosis on the other hand would result in respective increases. Interestingly inhibition of PI3-kinase by LY294002 in HEK cells inhibited only wild-type DRA but not DRA-ETKFminus, indicating that PI3-kinase maintains exocytic insertion of DRA into the plasma membrane. To address the observed interplay between lipid rafts and PI3-kinase, raft integrity was disrupted and PI3-kinase activity was inhibited simultaneously. The resulting inhibitory effect was not additive, suggesting that PI3-kinase and lipid rafts act along the same route with regard to DRA activity.

Based on these findings we suggest that DRA is present in lipid rafts in an intracellular fraction, for instance in recycling vesicles or vesicles moving from another compartment to the plasma membrane (Fig. 14). Insertion from this intracellular compartment requires the interaction with one (or several) PDZ adaptor proteins, raft integrity, and the action of PI3-kinase. Disruption of raft integrity or inhibition of PI3-kinase will both inhibit DRA activity in this model. At least in transfected cells alternative or additional routes to the plasma membrane must exist to explain why DRA-ETKFminus is active. Thus the described mechanism may primarily maintain order and/or specificity in the complex subapical processes of the absorptive enterocyte.

Our data and our interpretation of the role of the PDZ interaction in the process of recycling are supported by previous studies. Wente et al. (48) demonstrated that the internalization of the somatostatin receptor subtype 5 (SSTR5) as well as its targeting to Golgi-associated compartments are PDZ independent. However, the recycling of the receptor to the plasma membrane depends on PDZ adaptor proteins PIST (also known as GOPC or CAL) and PDZK1. In addition Swiatecka-Urban et al. (45) have shown that CFTR reinsertion into the plasma membrane but not retrieval from the plasma membrane requires the PDZ interaction.

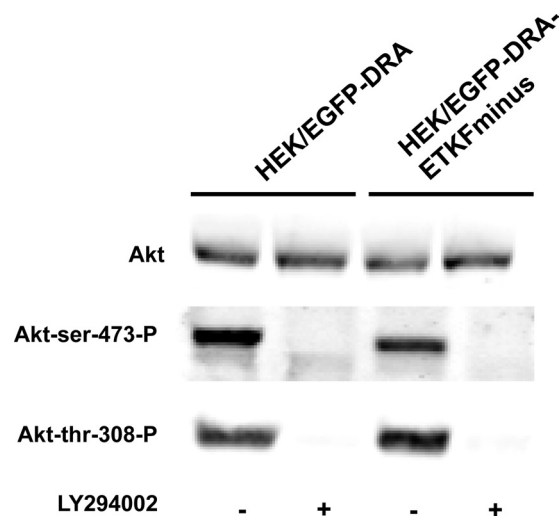


Fig. 10. Phosphorylation of Akt is inhibited by LY294002. HEK/EGFP-DRA (A) and HEK/EGFP-DRA-ETKFminus (B) cells were treated with 50 μ M LY294002 for 30 min at 37°C. Under control conditions both phosphorylation sites of Akt were phosphorylated. But in the presence of LY294002 the phosphorylation was abolished. Representative data of 3 experiments.

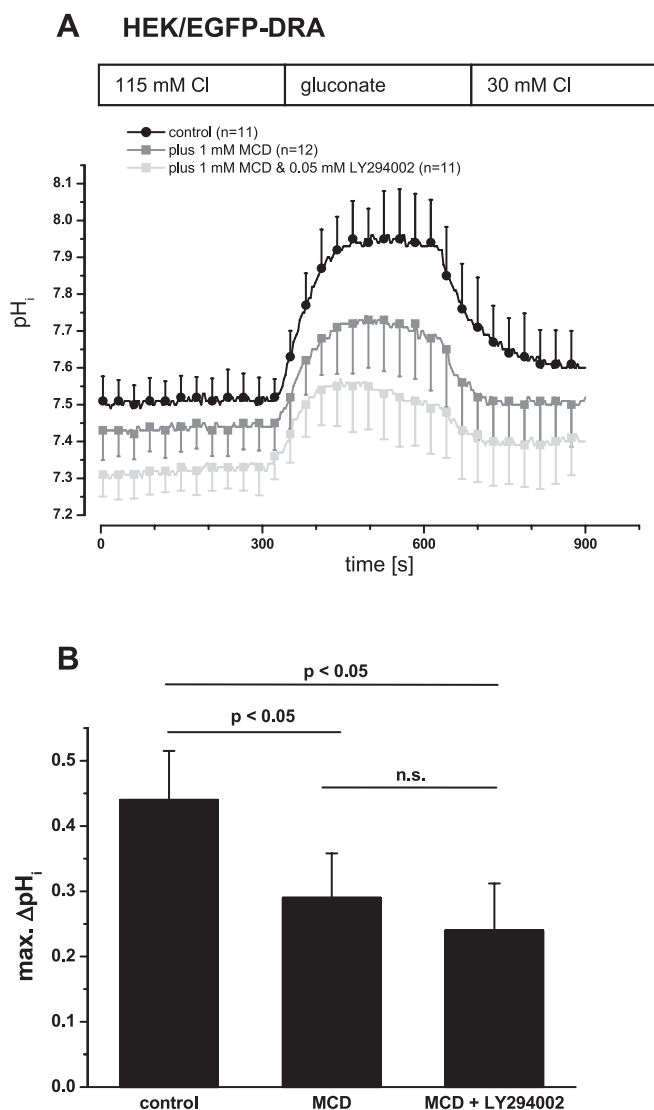


Fig. 11. Inhibition of PI3-kinase inhibits DRA by the same pathway as disruption of raft integrity. HEK/EGFP-DRA cells were treated with 1 mM MCD at 37°C for 60 min or with MCD and LY294002 (1 mM MCD, 37°C, 60 min; 50 μ M LY294002, 37°C, 30 min) prior to the functional experiment. **A:** simultaneous incubation with MCD and LY294002 did not further decrease DRA activity compared with the incubation with MCD alone. **B:** summary of the maximal (max.) pH_i change.

The involvement of PI3-kinase in the regulation of DRA has been shown in other studies as well. Lysophosphatidic acid and *Lactobacillus acidophilus* stimulate Cl/OH exchange and increase cell surface levels of DRA via a PI3-kinase-mediated mechanism (2, 44). So far lipid rafts as well as PDZ interactions have not been addressed in this process.

PDZK1 anchors (or facilitates retention of) NHE3 and a number of other transporters in the brush border membrane (1, 6, 19, 34, 46, 51). DRA and NHE3 as well as PDZK1 are associated with lipid rafts. Our data show that the lipid raft association of DRA is independent of its interaction with PDZ adaptor proteins and that the lipid raft localization of the PDZ adaptor proteins PDZK1, E3KARP, and IKEPP is independent of the expression of DRA. Thus DRA is not recruited to lipid rafts by any PDZ adaptor protein and vice versa. Nevertheless DRA and PDZK1 (as well as E3KARP and

IKEPP) strongly interact in lipid rafts and raft integrity is required for proper DRA function. Thus our data show an intriguing and previously unappreciated interplay between the PDZ interaction, the lipid raft association, and the activity of an apical transport protein. Given the wide distribution of PDZ interactions of transmembrane proteins and the increasing demonstration of their localization in lipid rafts it appears possible that such interplay may be more widespread. The cellular compartment where DRA and PDZK1 meet and where they travel as well as the possibility of the involvement of other PDZ adaptor proteins and other PDZ ligands will be a topic of future studies.

Taken together our data show, that a specific interaction of DRA with one or several PDZ adaptor proteins, most likely PDZK1, occurs in lipid rafts and that this interaction is essential for the exocytic PI3-kinase dependent insertion of DRA into the plasma membrane. Thereby the PDZ interaction of DRA aids in the building and maintenance of the complex, lipid raft including architecture of a polarized epithelial cell.

GRANTS

This work was supported by Deutsche Forschungsgemeinschaft Grants La 1066/3-1 and La 1066/3-2 and a grant from the Zentrum für Ernährungsmedizin 10A II-08.

DISCLOSURES

No conflicts of interest, financial or otherwise, are declared by the author(s).

REFERENCES

- Anzai N, Miyazaki H, Noshiro R, Khamdang S, Chairoungdua A, Shin HJ, Enomoto A, Sakamoto S, Hirata T, Tomita K, Kanai Y, Endou H. The multivalent PDZ domain-containing protein pdzk1 regulates transport activity of renal urate-anion exchanger URAT1 via its C terminus. *J Biol Chem* 279: 45942–45950, 2004.
- Borthakur A, Gill RK, Tyagi S, Koutsouris A, Alrefai WA, Hecht GA, Ramaswamy K, Dudeja PK. The probiotic lactobacillus acidophilus stimulates chloride/hydroxyl exchange activity in human intestinal epithelial cells. *J Nutr* 138: 1355–1359, 2008.
- Brown DA, Rose JK. Sorting of GPI-anchored proteins to glycolipid-enriched membrane subdomains during transport to the apical cell surface. *Cell* 68: 533–544, 1992.
- Brown DA. Lipid rafts, detergent-resistant membranes, and raft targeting signals. *Physiology* 21: 430–439, 2006.
- Buk DM, Waibel M, Braig C, Martens AS, Heinrich PC, Graeve L. Polarity and lipid raft association of the components of the ciliary neurotrophic factor receptor complex in Madin-Darby canine kidney cells. *J Cell Sci* 117: 2063–2075, 2004.
- Capuano P, Bacic D, Stange G, Hernando N, Kaissling B, Pal R, Kocher O, Biber J, Wagner CA, Murer H. Expression and regulation of the renal Na/phosphate cotransporter NaPi-IIa in a mouse model deficient for the PDZ protein PDZK1. *Pflügers Arch* 449: 392–405, 2005.
- Craven SE, El Husseini AE, Brecht DS. Synaptic targeting of the postsynaptic density protein PSD-95 mediated by lipid and protein motifs. *Neuron* 22: 497–509, 1999.
- Eshcol JO, Harding AM, Hattori T, Costa V, Welsh MJ, Benson CJ. Acid-sensing ion channel 3 (ASIC3) cell surface expression is modulated by PSD-95 within lipid rafts. *Am J Physiol Cell Physiol* 295: C732–C739, 2008.
- Field M. Intestinal ion transport and the pathophysiology of diarrhea. *J Clin Invest* 111: 931–943, 2003.
- Hanzal-Bayer MF, Hancock JF. Lipid rafts and membrane traffic. *FEBS Lett* 581: 2098–2104, 2007.
- Harder T, Scheiffelle P, Verkade P, Simons K. Lipid domain structure of the plasma membrane revealed by patching of membrane components. *J Cell Biol* 141: 929–942, 1998.
- Helms JB, Zurzolo C. Lipids as targeting signals: lipid rafts and intracellular trafficking. *Traffic* 5: 247–254, 2004.

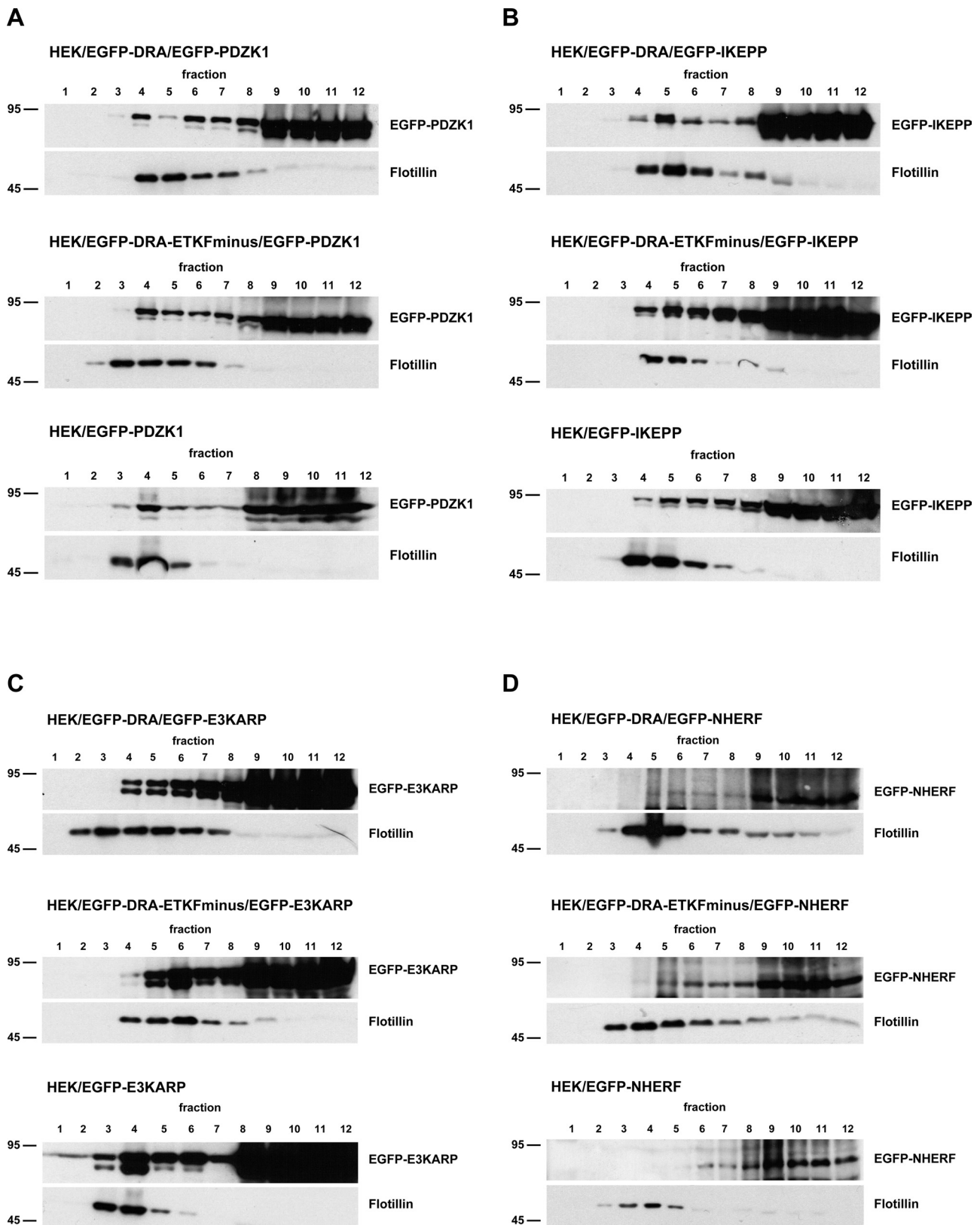


Fig. 12. PDZK1, IKEPP, and E3KARP but not NHERF are associated with lipid rafts. HEK/EGFP-DRA, HEK/EGFP-DRA-ETKFminus, and native HEK cells were transiently transfected with EGFP-PDZK1 (A), EGFP-IKEPP (B), EGFP-E3KARP (C), and EGFP-NHERF (D). The cells were solubilized in 1% Triton X-100 and the lysates were separated by sucrose gradient centrifugation. Expectedly, flotillin was detected in the low-density fractions EGFP-PDZK1 (A), EGFP-IKEPP (B), and EGFP-E3KARP (C) were detected in both low-density and high-density fractions in nontransfected and transfected HEK cells, indicating that they are partially associated with lipid rafts independently of their interaction with DRA. D: EGFP-NHERF was only detected in the high-density fractions and is apparently not associated with lipid rafts. Representative data of 5 experiments.

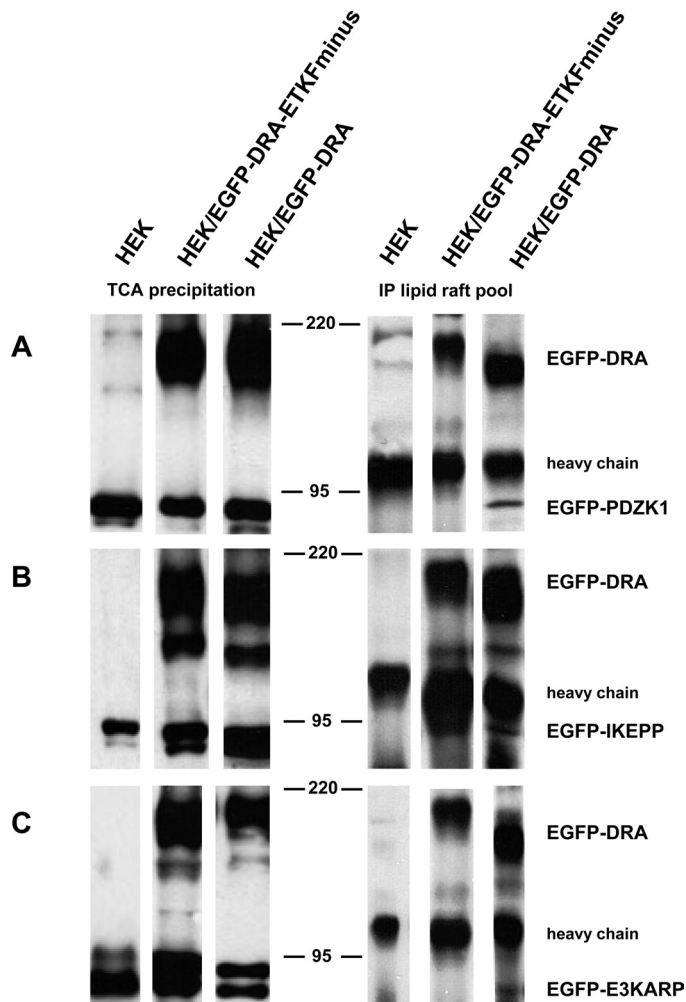


Fig. 13. DRA interacts with the PDZ adaptor proteins PDZK1, E3KARP, and IKEPP within lipid rafts. HEK/EGFP-DRA, HEK/EGFP-DRA-ETKfminus, and native HEK cells were transiently transfected with EGFP-PDZK1 (A), EGFP-IKEPP (B), and EGFP-E3KARP (C). *Left*: lipid raft fractions from the sucrose gradient were pooled, TCA precipitated, and tested for the presence of EGFP-DRA (or EGFP-DRA-ETKfminus) and the various EGFP-PDZ adaptor proteins by using a monoclonal anti-EGFP antibody. *Right*: the same pooled lipid raft fractions were subjected to immunoprecipitation (IP) using a polyclonal anti-DRA antibody. The immunoprecipitated material was tested for the successful precipitation of EGFP-DRA (or EGFP-DRA-ETKfminus) and for coimmunoprecipitation of the various EGFP-PDZ adaptor proteins by use of a monoclonal anti-EGFP antibody. Representative data of 3 experiments.

13. Hill WG, Butterworth MB, Wang H, Edinger RS, Lebowitz J, Peters KW, Frizzell RA, Johnson JP. The epithelial sodium channel (ENaC) traffics to apical membrane in lipid rafts in mouse cortical collecting duct cells. *J Biol Chem* 282: 37402–37411, 2007.
14. Hoglund P, Haila S, Socha J, Tomaszewski L, Saarialho-Kere U, Karjalainen-Lindsberg ML, Airola K, Holmberg C, de la Chapelle A, Kere J. Mutations of the Down-regulated in adenoma (DRA) gene cause congenital chloride diarrhoea. *Nat Genet* 14: 316–319, 1996.
15. Ikonen E. Roles of lipid rafts in membrane transport. *Curr Opin Cell Biol* 13: 470–477, 2001.
16. Ilangumaran S, Hoessli DC. Effects of cholesterol depletion by cyclodextrin on the sphingolipid microdomains of the plasma membrane. *Biochem J* 335: 433–440, 1998.
17. Itoh K, Sakakibara M, Yamasaki S, Takeuchi A, Arase H, Miyazaki M, Nakajima N, Okada M, Saito T. Cutting edge: negative regulation of immune synapse formation by anchoring lipid raft to cytoskeleton through Cbp-EBP50-ERM assembly. *J Immunol* 168: 541–544, 2002.
18. Jiang L, Fernandes D, Mehta N, Bean JL, Michaelis ML, Zaidi A. Partitioning of the plasma membrane Ca^{2+} -ATPase into lipid rafts in

- primary neurons: effects of cholesterol depletion. *J Neurochem* 102: 378–388, 2007.
19. Kato Y, Sai Y, Yoshida K, Watanabe C, Hirata T, Tsuji A. PDZK1 directly regulates the function of organic cation/carnitine transporter OCTN2. *Mol Pharmacol* 67: 734–743, 2004.
20. Lamprecht G, Baisch S, Schoenleber E, Gregor M. Transport properties of the human intestinal anion exchanger DRA (down regulated in adenoma) in transfected HEK293 cells. *Pflügers Arch* 449: 479–490, 2005.
21. Lamprecht G, Gaco V, Turner JR, Natour D, Gregor M. Regulation of the intestinal anion exchanger DRA (downregulated in adenoma). *Ann NY Acad Sci* 1165: 261–266, 2009.
22. Lamprecht G, Heil A, Baisch S, Lin-Wu E, Yun CC, Kalbacher H, Gregor M, Seidler U. The down regulated in adenoma (dra) gene product binds to the second PDZ domain of the NHE3 kinase A regulatory protein (E3KARP), potentially linking intestinal Cl^{-}/HCO_3^{-} exchange to Na^{+}/H^{+} exchange. *Biochemistry* 41: 12336–12342, 2002.
23. Lamprecht G, Seidler U. The emerging role of PDZ adapter proteins for regulation of intestinal ion transport. *Am J Physiol Gastrointest Liver Physiol* 291: G766–G777, 2006.
24. Lamprecht G, Hsieh CJ, Lissner S, Nold L, Heil A, Gaco V, Schafer J, Turner JR, Gregor M. The intestinal anion exchanger down regulated in adenoma (DRA) is inhibited by intracellular calcium. *J Biol Chem* 284: 19744–19753, 2009.
25. Lamprecht G, Schaefer J, Dietz K, Gregor M. Chloride and bicarbonate have similar affinities to the intestinal anion exchanger DRA (down regulated in adenoma). *Pflügers Arch* 452: 307–315, 2006.
26. Li X, Leu S, Cheong A, Zhang H, Baibakov B, Shih C, Birnbaum M, Donowitz M. Akt2, phosphatidylinositol 3-kinase, and PTEN are in lipid rafts of intestinal cells: role in absorption and differentiation. *Gastroenterology* 126: 122–135, 1993.
27. Li X, Galli T, Leu S, Wade JB, Weinman EJ, Leung G, Cheong A, Louvard D, Donowitz M. Na^{+}/H^{+} exchanger 3 (NHE3) is present in lipid rafts in the rabbit ileal brush border: a role for rafts in trafficking and rapid stimulation of NHE3. *J Physiol* 537: 537–552, 2001.

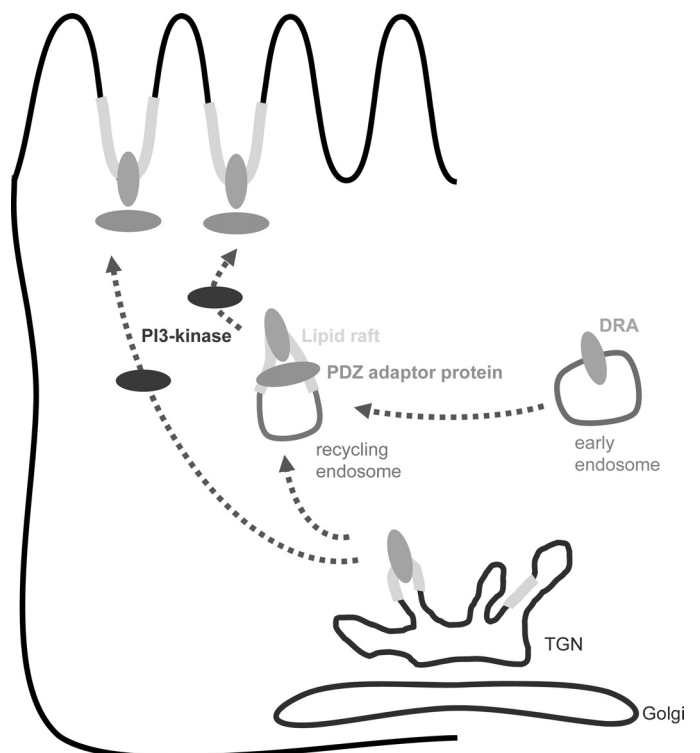


Fig. 14. Working model for exocytic trafficking of DRA and the role of lipid rafts, PI3-kinase, and PDZ adaptor proteins. PI3-kinase is required for insertion of DRA into the plasma membrane. DRA is present in lipid rafts even before the action of PI3-kinase takes place. DRA interacts with one or several PDZ adaptor proteins in lipid rafts, and this interaction is required for exocytosis of DRA. TGN, trans-Golgi network.

28. Lindmo K, Stenmark H. Regulation of membrane traffic by phosphoinositide 3-kinases. *J Cell Sci* 119: 605–614, 2006.
29. Ma L, Huang YZ, Pitcher GM, Valtschanoff JG, Ma YH, Feng LY, Lu B, Xiong WC, Salter MW, Weinberg RJ, Mei L. Ligand-dependent recruitment of the erbB4 signaling complex into neuronal lipid rafts. *J Neurosci* 23: 3164–3175, 2003.
30. Magnani F, Tate CG, Wynne S, Williams C, Haase J. Partitioning of the serotonin transporter into lipid microdomains modulates transport of serotonin. *J Biol Chem* 279: 38770–38778, 2004.
31. Martens JR, Sakamoto N, Sullivan SA, Grobaski TD, Tamkun MM. Isoform-specific localization of voltage-gated K⁺ channels to distinct lipid raft populations. *J Biol Chem* 276: 8409–8414, 2001.
32. Murtazina R, Kovbasnjuk O, Donowitz M, Li X. Na⁺/H⁺ exchanger NHE3 activity and trafficking are lipid raft-dependent. *J Biol Chem* 281: 17845–17855, 2006.
33. Nguyen HTT, Charrier-Hisamuddin L, Dalmasso G, Hiol A, Sitaraman S, Merlin D. Association of PepT1 with lipid rafts differently modulates its transport activity in polarized and nonpolarized cells. *Am J Physiol Gastrointest Liver Physiol* 293: G1155–G1165, 2007.
34. Noshiro R, Anzai N, Sakata T, Miyazaki H, Terada T, Shin HJ, He X, Miura D, Inui K, Kanai Y, Endou H. The PDZ domain protein PDZK1 interacts with human peptide transporter PEPT2 and enhances its transport activity. *Kidney Int* 70: 275–282, 2006.
35. Pierce SK. Lipid rafts and B-cell activation. *Nat Rev Immunol* 2: 96–105, 2002.
36. Rietveld A, Simons K. The differential miscibility of lipids as the basis for the formation of functional membrane rafts. *Biochim Biophys Acta* 1376: 467–479, 1998.
37. Roepstorff K, Thomsen P, Sandvig K, van Deurs B. Sequestration of epidermal growth factor receptors in non-caveolar lipid rafts inhibits ligand binding. *J Biol Chem* 277: 18954–18960, 2002.
38. Ruppelt A, Mosenden R, Gronholm M, Aandahl EM, Tobin D, Carlson CR, Abrahamsen H, Herberg FW, Carpen O, Tasken K. Inhibition of T cell activation by cyclic adenosine 5'-monophosphate requires lipid raft targeting of protein kinase A type I by the A-kinase anchoring protein ezrin. *J Immunol* 179: 5159–5168, 2007.
39. Salzer U, Prohaska R. Stomatin, flotillin-1, and flotillin-2 are major integral proteins of erythrocyte lipid rafts. *Blood* 97: 1141–1143, 2001.
40. Schultheis PJ, Clarke LL, Meneton P, Miller ML, Soleimani M, Gawenis LR, Riddle TM, Duffy JJ, Doetschman T, Wang T, Giebisch G, Aronson PS, Lorenz JN, Shull GE. Renal and intestinal absorptive defects in mice lacking the NHE3 Na⁺/H⁺ exchanger. *Nat Genet* 19: 282–285, 1998.
41. Schweinfest CW, Spyropoulos DD, Henderson KW, Kim JH, Chapman JM, Barone S, Worrell RT, Wang Z, Soleimani M. slc26a3 (dra)-deficient mice display chloride-losing diarrhea, enhanced colonic proliferation, and distinct up-regulation of ion transporters in the colon. *J Biol Chem* 281: 37962–37971, 2006.
42. Shogomori H, Brown DA. Use of detergents to study membrane rafts: the good, the bad, and the ugly. *Biol Chem* 384: 1259–1263, 2003.
43. Simons K, Toomre D. Lipid rafts and signal transduction. *Nat Rev Mol Cell Biol* 1: 31–39, 2000.
44. Singla A, Dwivedi A, Saksena S, Gill RK, Alrefai WA, Ramaswamy K, Dudeja PK. Mechanisms of lysophosphatidic acid (LPA) mediated stimulation of intestinal apical Cl⁻/OH⁻ exchange. *Am J Physiol Gastrointest Liver Physiol* 298: G182–G189, 2010.
45. Swiatecka-Urban A, Duhaime M, Coutermarsh B, Karlson KH, Collawn J, Milewski M, Cutting GR, Guggino WB, Langford G, Stanton BA. PDZ domain interaction controls the endocytic recycling of the cystic fibrosis transmembrane conductance regulator. *J Biol Chem* 277: 40099–40105, 2002.
46. Wang S, Yue H, Derin RB, Guggino WB, Li M. Accessory protein facilitated CFTR-CFTR interaction, a novel molecular mechanism to potentiate the chloride channel activity. *Cell* 103: 169–179, 2000.
47. Welker P, Bohlick A, Mutig K, Salanova M, Kahl T, Schluter H, Blottner D, Ponce-Coria J, Gamba G, Bachmann S. Renal Na⁺-K⁺-Cl⁻ cotransporter activity and vasopressin-induced trafficking are lipid raft-dependent. *Am J Physiol Renal Physiol* 295: F789–F802, 2008.
48. Wente W, Stroth T, Beaudet A, Richter D, Kreienkamp HJ. Interactions with PDZ domain proteins PIST/GOPC and PDZK1 regulate intracellular sorting of the somatostatin receptor subtype 5. *J Biol Chem* 280: 32419–32425, 2005.
49. Wong W, Schlichter LC. Differential recruitment of Kv1.4 and Kv4.2 to lipid rafts by PSD-95. *J Biol Chem* 279: 444–452, 2004.
50. Yun CHC, Oh S, Zizak M, Steplock D, Tsao S, Tse CM, Weinman EJ, Donowitz M. cAMP-mediated inhibition of the epithelial brush border Na⁺/H⁺ exchanger, NHE3, requires an associated regulatory protein. *Proc Natl Acad Sci USA* 94: 3010–3015, 1997.
51. Zachos NC, Li X, Kovbasnjuk O, Hogema B, Sarker R, Lee LJ, Li M, de Jonge H, Donowitz M. NHERF3 (PDZK1) contributes to basal and calcium inhibition of NHE3 activity in Caco-2BBE cells. *J Biol Chem* 284: 23708–23718, 2009.